OPEN

Correspondence and
requests for materials
should be addressed to
X.P.L. (mpelixp@nus.
eud.sg)

The Dynamic Dielectric at a Brain Functional Site and an EM Wave Approach to Functional Brain Imaging

X. P. Li[1], Q. Xia[2], D. Qu[1], T. C. Wu[1], D. G. Yang[3], W. D. Hao[3], X. Jiang[3] & X. M. Li[3]

[1]Neuroengineering Lab, National University of Singapore, 9 Engineering Drive 1, Singapore 117575, [2]Newrocare Pte Ltd, 6 EU Tong Sen Street, #12-03, The Central, Singapore 059817, [3]Guilin University of Electronic Technology, No.1 Jinji Road, Guilin 541004, Guangxi, P.R. China.

Functional brain imaging has tremendous applications. The existing methods for functional brain imaging include functional Magnetic Resonant Imaging (fMRI), scalp electroencephalography (EEG), implanted EEG, magnetoencephalography (MEG) and Positron Emission Tomography (PET), which have been widely and successfully applied to various brain imaging studies. To develop a new method for functional brain imaging, here we show that the dielectric at a brain functional site has a dynamic nature, varying with local neuronal activation as the permittivity of the dielectric varies with the ion concentration of the extracellular fluid surrounding neurons in activation. Therefore, the neuronal activation can be sensed by a radiofrequency (RF) electromagnetic (EM) wave propagating through the site as the phase change of the EM wave varies with the permittivity. Such a dynamic nature of the dielectric at a brain functional site provides the basis for an RF EM wave approach to detecting and imaging neuronal activation at brain functional sites, leading to an RF EM wave approach to functional brain imaging.

The detection and imaging of neuronal activities in the brain has tremendous applications[1-4]. Several methods have been developed and studied extensively for such applications. For example, via measuring the BOLD signal[5,6], functional Magnetic Resonant Imaging (fMRI) has been used to capture human visual cortex activities[7], detect awareness of a brain in a vegetative state[8], image dopaminergic signals in the ventral tegmental area[9], and for general brain activity imaging purposes[10]. Scalp electroencephalography (EEG) has been developed for the brain-machine interface[11,12] and for detecting the area of onset of epilepsy[13]. But the source localisation is an ill-imposed inverse problem that has not been successfully solved[14,15]. With the advancement in methods of source localisation for magnetoencephalography (MEG), MEG has been used to localise functional areas of the cortex[16], and has been applied clinically for screening and diagnosis of post-traumatic stress disorder[17]. More effective but also more invasive, implanted EEG has been used on animals as a brain-machine interface[18,19] as well as on humans for detecting the area of onset of epilepsy[20] and for functional imaging of the amygdala[21].

Recently, the possibility of using radiofrequency (RF) electromagnetic (EM) waves for diagnosing stroke has been studied[22,23], and based on the significant dielectric property differences between brain tissues and blood, cerebral haemorrhage has been diagnosed and localised with a multi-channel RF EM wave propagating through haemorrhaged brain compared to a normal brain. In similar concepts, RF EM wave based radiometry has been studied for non-invasive brain temperature monitoring[24], and a novel RF EM wave tomography system has been developed for experimental breast imaging[25].

In this study, we aimed to develop an active, non-invasive method for detecting and imaging neuronal activations in the brain, through studying the biophysics of an activated functional site in the brain and its relationship to an externally applied RF EM field. We first hypothesised that neuronal activation at a functional site in the brain varies the ion concentration of the extracellular fluid surrounding the activated neurons, and thus varies the permittivity of the dielectric (extracellular fluid) at the functional site; an RF EM wave propagating through the activated functional site will be changed and the change varies with the variation of the permittivity of the dielectric, and thus varies with neuronal activation at the functional site. We then validated the hypothesis with an RF EM wave experiment on a rat brain monitored with simultaneous EEG measurement, and we obtained results confirming that the phase change or amplitude change of the RF EM wave propagating through a rat brain varies with the brain activity, providing the basis for a RF EM wave approach to functional brain imaging.

The extracellular fluid surrounding the neurons at a functional site in the brain is a typical dielectric by ionic polarisation. At a brain functional site, the ion concentration in the extracellular fluid varies with local neuronal activation[26,27], which indicates the dynamic nature of the dielectric at the functional site. Also, the ion concentration of the extracellular fluid surrounding the neurons at a functional site in the brain varies with neuronal activation - repolarisation and depolarisation (Fig. 1(A) and (B)) in which synchronised neuronal activations give rise to immense transmembrane ion flows, changing the ion concentration of the extracellular fluid, and therefore, changing the permittivity. Varying the ion concentration results in a dynamic permittivity of the dielectric (the extracellular fluid), and under an externally applied electric field, E, the energy taken from the applied field and stored in the dielectric in forming a polarisation density, P, varies according to the neuronal activation status from P_S during the synchronised neuronal activation in repolarisation to P_w during the synchronised neuronal activation in depolarisation (Fig. 1(C) and (D)) and then back to P_S, and so on.

Theoretically, when a monochrome plane EM wave propagates normally into a nonlinear dielectric body of multi-layer low-loss material, such as the brain, the amplitude and phase of the propagating EM wave are changed according to the permittivity of the dielectric (the extracellular fluid). In this study, we derived the relationship between the EM wave phase change, φ, and the value of the permittivity of the dielectric, ε, by applying the planar transmission mode[28]

to the phase change of the EM wave between a pair of transmitting and receiving waveguides, as:

$$\varphi = \sum_{i=1}^{n} \beta_i(\varepsilon)l_i + \sum_{j=1}^{m} ArgT_j(\varepsilon) \qquad (1)$$

where $\beta_i(\varepsilon)$ is the phase constant of the ith layer, l_i is the propagating path length of the ith layer, and $ArgT_j(\varepsilon)$ is the phase of the transmission coefficient of the jth interface. Both $\beta_i(\varepsilon)$ and $T_j(\varepsilon)$ are functions of the permittivity or polarisation density of the dielectric. It should be noted that Equation (1) was derived according to the assumption of the EM wave propagating through an infinite planar medium, which is not exactly the case for an EM wave propagating through the brain in between a transmitting waveguide and a receiving waveguide in the present study. However, because the EM wave applied in the present study is a millimeter wave and the waveguide's dimension (7.11 mm $\times$ 3.56 mm) is smaller than the brain size of rats (approximately 16 mm from the left to the right, 12 mm from the front to the back, and 10 mm from the top to the bottom) used in the present study, the transmission mode is approximated according to the planar transmission mode in which the law that the phase of the EM wave propagating through a dielectric varies qualitatively with the permittivity of the dielectric is truly represented.

To confirm the analysis, we used software CST2011 of CST - Computer Simulation Technology AG to simulate the phase change of a 30 GHz EM wave propagating through a rat head with neuronal
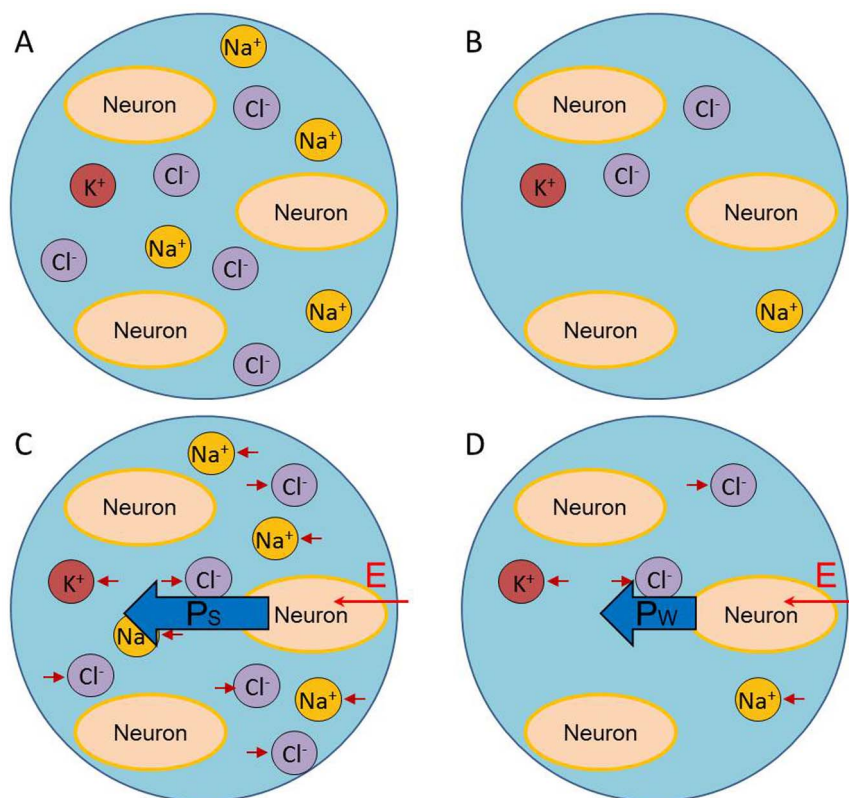

Figure 1 | The neuronal activation at a brain functional site gives rise to immense transmembrane ion flows, varying the ion concentration of the extracellular fluid at the functional site, and therefore, varying the permittivity of the fluid. (A) When the neurons are in synchronised depolarisation, their membranes pump sodium ions out and largely increase the ion concentration in the surrounding extracellular fluid. (B) When the neurons are in synchronised depolarisation, many sodium ions rush into the neuronal cell bodies and largely reduce the ion concentration of the extracellular fluid. (C) Under an applied electric field, E (shown with a small red arrow indicating the field direction), a strong polarisation density, P_S, is formed in the extracellular fluid at the functional site when the neurons are in synchronised depolarisation and result in a high ion concentration of the extracellular fluid. (D) Also, under the applied electric field, E (shown with a small red arrow indicating the field direction), a weak polarisation density, P_w, is formed in the extracellular fluid at the neuronal activation site when the neurons are in synchronised repolarisation and result in a low ion concentration of the extracellular fluid.
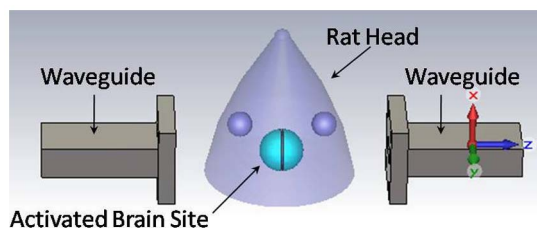
Figure 2 | Simulation setup, showing the 3D geometry of the simulated rat head, geometry and location of the simulated activated brain site, and waveguides assumed in the simulation, where the rat brain sizes were 16 mm from the left to the right, 12 mm from the front to the back, and 10 mm from the top to the bottom, the transmitting waveguide on the left was 10 mm away from the left side of the brain, the receiving waveguide on the right was 10 mm away from the right side of the brain, and each of the waveguides was a rectangular hollow metallic waveguide of 7.11 mm × 3.56 mm.

activation such that the permittivity varies. The 3D geometry of the simulated rat head, geometry and location of the simulated activated brain site, and waveguides assumed in the simulation are shown in Figure 2. The material properties of the simulated head are shown in Table 1; the values are given for human heads because data for rat heads under a 30 GHz EM wave were not available. The simulation results, as shown in Figure 3, indicate that as the relative permittivity at the activated brain site (approximately spherical with the radius R = 6 mm) was increased from 22 to 44, the phase change arg(S2,1) of the EM wave increased from 53.39° to 53.92°. When the volume of the activated brain site was decreased by 96.3% (approximately spherical with the radius R = 2 mm), as the relative permittivity at the activated brain site was increased from 22 to 44, the phase change arg(S2,1) of the EM wave increased from 52.76° to 52.95°.

The analysis and simulation can be used to develop a theory regarding the dynamic nature of the permittivity of the dielectric at brain functional sites. We based the theory on a RF EM wave approach to functional brain imaging. To develop the theory, we hypothesised that:

1. The volume of extracellular fluid at a functional brain site is the dielectric that has the same ionic polarisation as the RF EM wave propagating through it, in which the ions (Na^+, K^+, Mg^{2+}, Ca^{2+}, Cl^-, etc.) surrounding the neurons are pushed or pulled by the EM field. As a result of losing energy to the volume of extracellular fluid, the propagating EM wave changes its amplitude and phase.
2. As a functional brain site has activity, the activation of the neurons (synchronised at a frequency) periodically varies the ion concentration in the volume of the extracellular fluid and the permittivity of the fluid varies correspondingly, resulting in variation in the EM field energy loss, and consequently, variation in the EM wave amplitude and phase changes.
3. By measuring the variation of the amplitude change or phase change of a RF EM wave propagating through a brain functional site in activation, the neuronal activation can be sensed and characterised.

To validate the hypothesis, we conducted experiments on RF EM wave detection of rat brain neuronal activities in a microwave anechoic chamber of EM shielding efficiency above 90 dB at 18 to
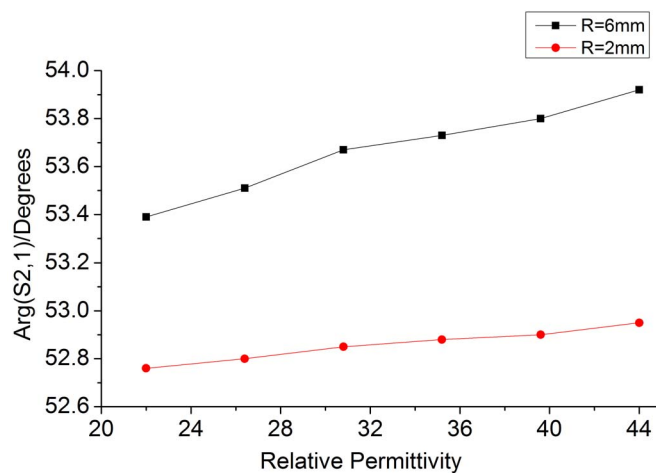

Figure 3 | Simulation result showing the variation in the phase change arg(S2,1) of the 30 GHz EM wave propagating through an activated brain site vs the variation of the relative permittivity of the dielectric at the brain site. The approximately spherical, activated brain site with a radius R = 6 mm exhibited the variation of EM wave phase change, which increased from 53.39° to 53.92° when the relative permittivity of dielectric at the activated brain increased from 22 to 44. The approximately spherical, activated brain site with a radius R = 2 mm exhibited the variation of EM wave phase change, which increased from 52.76° to 52.95° when the relative permittivity of dielectric at the activated brain increased from 22 to 44.

40 GHz. Also, we used a 2-port Vector Network Analyzer (Agilent Technologies N5230A) transmitting 30 GHz of sinusoidal EM wave of -10 dBm by a waveguide at about 1 cm distance from the left side through the rat brain, which was received on the right side by another waveguide at about 1 cm from the rat brain, as shown in Figure 4. Each of the waveguides was a rectangular hollow metallic waveguide of 7.11 mm × 3.56 mm. There was nothing but air between the waveguide and rat head. Ten Sprague-Dawley rats were included in the experimental tests. During each test, the rat was kept anesthetised with inhalation of ether so that its head remained stationary. The variation of the phase and amplitude of the EM wave propagating through the rat brain was displayed on the screen of the analyser with the digital data saved for analysis. Simultaneous, one-channel scalp EEG recording was carried out to validate the variations in the EM wave phase and amplitude changes in relation to the rat neuronal activation. The signal acquisition electrode, reference electrode and earth electrode were placed on the lambda, eye socket, and body, respectively. For each test, the measurement recording time was 10 seconds. Both the recorded EM wave variation and EEG signal were analysed using FFT for comparison to confirm that the measured EM wave variation was associated with the rat brain neuronal activation, in which a recording of 5 seconds was used for the FFT on each test result. For further confirmation, in the test on each rat, the correlation between the variation of phase change of the EM wave propagating through the rat brain and the EEG signal was analysed with a linear correlation method, using 5 second epochs. Before the analyses, the noise and artefacts were removed using butterworth filters (order = 4, low-pass 20 Hz, high-pass 0.5 Hz, and notch 50 Hz), where the notch 50 Hz filter was used together with the low-pass

Table 1 | The material properties[31] of the simulated head

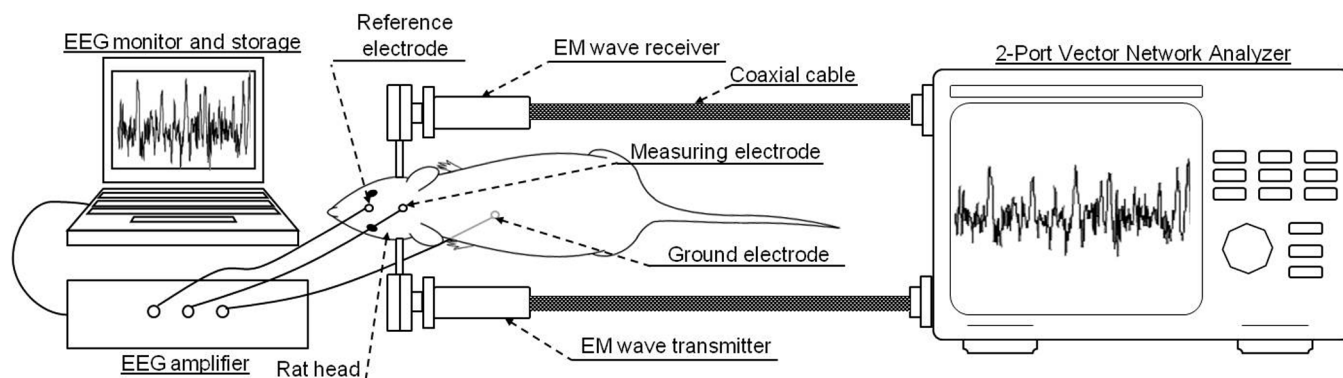|	Electrical Conductivity (f = 30 GHz)	Relative Permittivity (f = 30 GHz)	Weighted Components
Brain	27.2	17.2	(Grey Matter + White Matter)/2
ELSE	16.0	11.4	{Skin*1.5 + [(Muscle + Fat*2)/3]*4.5 + Bone*0.3}/6.3

Figure 4 | Experimental setup, where a rat, anesthetised with ether, was placed with the head centred in between the transmitting waveguide and receiving waveguide of an Agilent N5230A PNA-L 2 Port Vector Network Analyzer that was transmitting, receiving and analysing the variation of the EM wave propagating through the rat brain via an EEG electrode attached on the lambda, a reference electrode attached to the eye socket, and a ground electrode attached on the body. The electrodes were connected to an ANT EEG amplifier for acquiring EEG simultaneously with the EM wave measurement. This figure was drawn by TCW.

20 Hz filter because the low-pass filter could not fully remove artifacts originated from the power supply and therefore the notch filter was needed and applied.

The results from tests on the first rat (R1) are shown in Figure 5, where the left parts of (A) and (B) show the variations of the EM wave phase change and amplitude change, respectively, in the range of 0.1 to 0.3 degrees and 0.0003 to 0.0004 dB, respectively, as the RF EM wave propagated through the rat brain, and the right parts of (A) and (B) show the spectral densities for the variations of the EM wave phase change and amplitude change, respectively; the left part of (C) shows the simultaneous recorded EEG signal, and the right part of (C) shows the spectral densities for the EEG. The phase change and amplitude change of the EM wave varied as the EM wave propagated

through the rat brain, and the dominant variation frequency was 2.2 Hz. In comparison, the recorded EEG showed similar variation, and the dominant frequency was 2.2 Hz. The value of correlation between the variation of the phase change of the EM wave propagating through the rat brain and the EEG was 62.75%, which is significant considering that the EM wave variation reflected the entire brain's neuronal activation, whereas the one-channel EEG with a signal electrode measured only the electric potential at a point on the scalp, which did not cover some of the activated neuronal electrical sources, such as those having the dipole direction perpendicular to the lead vector with regard to the electrode location. In the EEG measurement for brain activities, the EEG waveform with a frequency ranging from 0.5 to 4 Hz is commonly categorised as
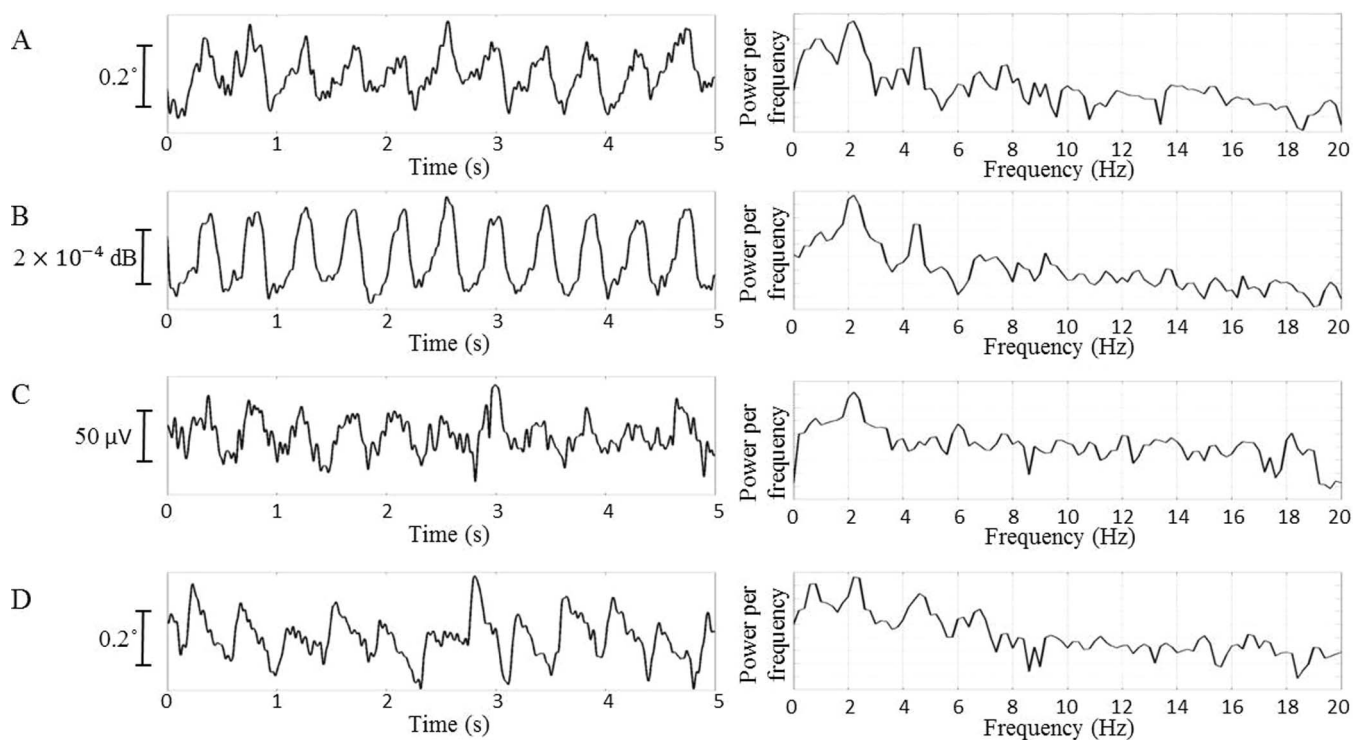

Figure 5 | Experimental results, where (A) shows the variation of the phase change of the EM wave propagating through the rat brain as well as the spectral density distribution. (B) The variation of amplitude change of the EM wave propagating through the rat brain and the spectral density distribution. (C) The EEG signal measured on the rat and the spectral density distribution. (D) After the EEG electrodes were removed from the rat, the variation of the phase change of the EM wave propagating through the rat brain and the spectral density distribution.

Table 2 | Correlation values of the variation of the phase change of the EM wave with the EEG signal

Rat	R1	R2	R3	R4	R5	R6	R7	R8	R9	R10
Correlation %	62.8	43.7	67.6	72.6	33.5	54.9	71.2	32.9	32.2	54.8

the Delta Wave[29], which is mainly associated with a slow-wave sleep mode of the brain. This was confirmed by comparing the EEG results with those obtained in a study by Terrier and Gottesmann[30], who performed comprehensive EEG studies on sleeping rats. During each of our tests, we observed that the rat was in a sleep mode, which was reasonable because the rat was anesthetised with inhalation of ether. Therefore, the variations of the phase change and amplitude change of the EM wave that propagated through the rat brain could be associated with the brain activities in a sleep mode.

To ensure that the EEG electrodes placed on the rat scalp and body as well as the EEG signal acquisition did not interfere with the measurement of the variation of the EM wave propagating through the rat brain, the EEG electrodes were then removed from the rat (R1), and the variation of the phase change of the EM wave propagating through the rat brain was measured again. As shown in Figure 5(D), the results were similar to those for simultaneous EEG measurement and recording, indicating that the electrodes and EEG signal acquisition did not interfere with the measurement of the variation of the EM wave propagating through the rat brain. This finding makes sense because the material properties of the electrodes did not change during the measurement, and the EEG signals had much lower frequencies than radiofrequencies and could not interfere with the EM wave. For the same reason that the EEG signals had much lower frequencies than the radiofrequencies, the EEG signal could not be affected by the RF EM instrumentation. We confirmed this through the EEG measurement with and without the RF EM wave measurement.

To confirm the results as shown in Figure 5, we used the same setup for measuring the variation of the EM wave propagating through the rat brain with simultaneous EEG measurement. Additional tests were performed on 9 more rats (R2 through R10). The results are shown in Supplementary Figure S1 online. In each of the tests, the EM wave phase variation was similar to the EEG signal, and the corresponding spectral densities had dominant frequencies in the same range of 0.5–4 Hz. Table 2 shows the values of the correlations between the variation of EM wave phase change and EEG signals for performing testing on all ten rats. The average correlation value is $52.62 \pm 15.25\%$, and the average correlation value for the pairs of unmatched variation of EM wave phase change and EEG signals (n=45) is $15.07 \pm 10.16\%$. The one tailed t-test, assuming equal variance (significance level 5%), indicates that correlations of the matched phase/EEG signal pairs are significantly greater than for the unmatched signal pairs (p=1e-13). This suggests that the observed high correlations between the variation of EM wave phase change and EEG signals were not from noise.

We have validated the hypothesis that the dielectric of a brain functional site has a dynamic nature associated to the local neuronal activation, indicating that neuronal activation is accessible by an RF EM wave. It is interesting that the simulation result of 0.53 degree of variation in the phase change, corresponding to a 100% variation in the relative permittivity of the dielectric, matches the experimental results of 0.2 to 0.6 degrees of variation in the phase change in the tests performed on ten rats, indicating that the relative permittivity of the dielectric at the activated brain sites might have varied for 36% to 107% during the neuronal activation in the ten rats. The variation of permittivity of the dielectric at a brain functional site following neuronal activation causes the variation of the phase change in the EM wave propagating through the brain. By measuring the variation

of the EM wave phase change, the neuronal activation can be measured.

Our finding of the dynamic nature of the dielectric at a brain functional site provides the basis for an RF EM wave approach to functional brain imaging, which is active (behaviour of the applied RF EM wave in relation to the measured neuronal activations), non-invasive, and utilises a simple hardware architecture (as simple as a mobile phone), functioning for both transmitting and receiving as well as processing the RF EM wave variation with neuronal activation at a brain functional site, in which neuronal activation at a particular functional site can be recognised based on that the permittivity of the dielectric at a functional site is frequency dependent, which reaches a maximum at a sensitive frequency associated with the functional site. By knowing the sensitive frequency of a functional site in the brain, detecting neuronal activations at the functional site with the RF EM wave approach can be similar to tuning a radio to a particular frequency band of a targeted radio station, which does not have the spatial resolution issues as in scalp EEG or the temporal resolution issues as in fMRI.

1. deCharms, R. C. Applications of real-time fMRI. *Nat Rev Neurosci* **9**, 720–729 (2008).
2. Michel, C. M. & Murray, M. M. Towards the utilization of EEG as a brain imaging tool. *Neuroimage* **61**, 371–385 (2012).
3. Heekeren, H. R., Marrett, S. & Ungerleider, L. G. The neural systems that mediate human perceptual decision making. *Nat Rev Neurosci* **9**, 467–479 (2008).
4. Farah, M. J., Hutchinson, J. B., Phelps, E. A. & Wagner, A. D. Functional MRI-based lie detection: scientific and societal challenges. *Nat Rev Neurosci* **15**, 123–131 (2014).
5. Mukamel, R. *et al.* Coupling between neuronal firing, field potentials, and FMRI in human auditory cortex. *Science* **309**, 951–954 (2005).
6. Lee, J. H. *et al.* Global and local fMRI signals driven by neurons defined optogenetically by type and wiring. *Nature* **465**, 788–792 (2010).
7. Engel, S. A. *et al.* fMRI of human visual cortex. *Nature* **369**, 525–525 (1994).
8. Owen, A. M. Detecting awareness in the vegetative state. *Science* **313**, 1402 (2006).
9. D'Ardenne, K., McClure, S. M., Nystrom, L. E. & Cohen, J. D. BOLD responses reflecting dopaminergic signals in the human ventral tegmental area. *Science* **319**, 1264–1267 (2008).
10. Kay, K. N. Identifying natural images from human brain activity. *Nature* **452**, 352–355 (2008).
11. Tomioka, R. & Muller, K. R. A regularized discriminative framework for EEG analysis with application to brain-computer interface. *Neuroimage* **49**, 415–432 (2010).
12. Nasseroleslami, B., Lakany, H. & Conway, B. A. EEG signatures of arm isometric exertions in preparation, planning and execution. *Neuroimage* **90**, 1–14 (2014).
13. Rullmann, M. *et al.* EEG source analysis of epileptiform activity using a 1 mm anisotropic hexahedra finite element head model. *Neuroimage* **44**, 399–410 (2009).
14. Strobbe, G. *et al.* Bayesian model selection of template forward models for EEG source reconstruction. *Neuroimage* **93**, 11–22 (2014).
15. Gramfort, A., Strohmeier, D., Haueisen, J., Hamalainen, M. S. & Kowalski, M. Time-frequency mixed-norm estimates: sparse M/EEG imaging with non-stationary source activations. *Neuroimage* **70**, 410–422 (2013).
16. Pang, E. W., Wang, F., Malone, M., Kadis, D. S. & Donner, E. J. Localization of Broca's area using verb generation tasks in the MEG: Validation against fMRI. *Neurosci Lett* **490**, 215–219 (2011).
17. Huang, M. X. *et al.* Voxel-wise resting-state MEG source magnitude imaging study reveals neurocircuitry abnormality in active-duty service members and veterans with PTSD. *Neuroimage Clin* **5**, 408–419 (2014).
18. Chapin, J. K., Moxon, K. A., Markowitz, R. S. & Nicolelis, M. A. Real-time control of a robot arm using simultaneously recorded neurons in the motor cortex. *Nat Neurosci* **2**, 664–670 (1999).
19. Wessberg, J. *et al.* Real-time prediction of hand trajectory by ensembles of cortical neurons in primates. *Nature* **408**, 361–365 (2000).
20. Cho, J. H. *et al.* Localization of ictal onset zones in Lennox-Gastaut syndrome (LGS) based on information theoretical time delay analysis of intracranial electroencephalography (iEEG). *Epilepsy Res* **99**, 78–86 (2012).
21. Murray, R. J., Brosch, T. & Sander, D. The functional profile of the human amygdala in affective processing: Insights from intracranial recordings. *Cortex* (2014).
22. Korfhagen, J. J., Kandadai, M. A., Clark, J. F., Adeoye, O. & Shaw, G. J. A prototype device for non-invasive continuous monitoring of intracerebral hemorrhage. *J Neurosci Methods* **213**, 132–137 (2013).
23. Persson, M. *et al.* Microwave-based stroke diagnosis making global pre-hospital thrombolytic treatment possible. *Biomedical Engineering, IEEE Transactions on* **PP**, 1–1 (2014).

24. Stauffer, P. R. *et al.* Non-invasive measurement of brain temperature with microwave radiometry: demonstration in a head phantom and clinical case. *Neuroradiol J* **27**, 3–12 (2014).

25. Meaney, P. M. *et al.* Initial clinical experience with microwave breast imaging in women with normal mammography. *Acad Radiol* **14**, 207–218 (2007).

26. Makarewicz, D. *et al.* NMDA-induced 45Ca release in the dentate gyrus of newborn rats: in vivo microdialysis study. *Neurochem Int* **37**, 307–316 (2000).

27. Takeda, A., Imano, S., Itoh, H. & Oku, N. Zinc release in the lateral nucleus of the amygdala by stimulation of the entorhinal cortex. *Brain Res* **1118**, 52–57 (2006).

28. Hayt, W. H. & Buck, J. A. *Engineering Electromagnetics.* 6th edn (*MacGraw-Hill*, New York, 2001).

29. Niedermeyer, H. & Lopes da Silva, F. H. *Electroencephalography: Basic Principles, Clinical Applications, and Related Fields.* 5th edn (*Williams & Wilkins*, Baltimore, 1999).

30. Terrier, G. & Gottesmann, C. L. Study of cortical spindles during sleep in the rat. *Brain Res Bull* **3**, 701–706 (1978).

31. Gabriel, S., Lau, R. W. & Gabriel, C. The dielectric properties of biological tissues: III. Parametric models for the dielectric spectrum of tissues. *Phys Med Biol* **41**, 2271 (1996).

Author contributions

X.P.L. designated the study, designed and executed experiments, analysed data and wrote the paper; Q.X. contributed the principal ideas; Q.D. executed experiments and simulated electromagnetic wave phase variation with the relative permittivity of the brain; T.C.W. processed and analysed the electromagnetic wave variation and EEG data; D.G.Y. coordinated and executed experiments and analysis; W.D.H. executed experiments and analysis; J.X. confirmed the theoretical analysis on EM wave phase variation with the permittivity of dielectric; X.M.L. collected EM wave variation data and simulated the electromagnetic fields. All authors discussed the results and commented on the manuscript.

Additional information

Supplementary information accompanies this paper at http://www.nature.com/scientificreports

Competing financial interests: The authors declare no competing financial interests.

How to cite this article: Li, X.P. *et al.* The Dynamic Dielectric at a Brain Functional Site and an EM Wave Approach to Functional Brain Imaging. *Sci. Rep.* **4**, 6893; DOI:10.1038/srep06893 (2014).